Electronic Supporting Information

Cholesterol appended bis-1,2,3-triazoles as simple supramolecular gelators for naked eye detection of Ag^+, Cu^{2+} and Hg^{2+} ions

Kumaresh Ghosh*, **Atanu Panja and Santanu Panja**

Department of Chemistry, University of Kalyani, Kalyani-741235, India.
Email: ghosh_k2003@yahoo.co.in

Table S1. Results of gelation test for **1-5**.

Solvents	**1**	**2**	**3**	**4**	**5**
$CHCl_3$	S	S	S	S	S
2% CH_3OH in $CHCl_3$	S	S	S	S	S
$CHCl_3$: CH_3OH (1:1, v/v)	P	P	P	PG	S
$CHCl_3$: CH_3OH (2:1, v/v)	G	G	G	S	S
$CHCl_3$: CH_3OH (3:1, v/v)	S	S	S	S	S
$CHCl_3$: Pet ether (1:1, v/v)	PS	PS	PS	S	S
CH_3COCH_3	I	I	I	PS	S
DMF	PG	PG	PG	PS	S
DMF:H_2O (1:1, v/v)	P	P	P	P	P
CH_3CN	I	I	I	PS	S
CH_3CN : $CHCl_3$ (1:1, v/v)	S	S	S	S	S
CH_3OH	I	I	PS	PS	PS
CH_3OH :H_2O (1:1, v/v)	I	I	I	I	P
DMSO	I	I	PS	PS	S
1% DMSO in CH_3CN	I	I	I	PS	S
Diethyl ether	I	I	PS	PS	S
Cyclohexane	I	I	I	PS	S

S = solution, G = gel (minimum gelation concentration; **1** = 14.6 mg/mL, **2** = 13.5 mg/mL, **3** = 12.2 mg/mL), I= insoluble, PG = partial gelation, PS = partial soluble, P = precipitation.

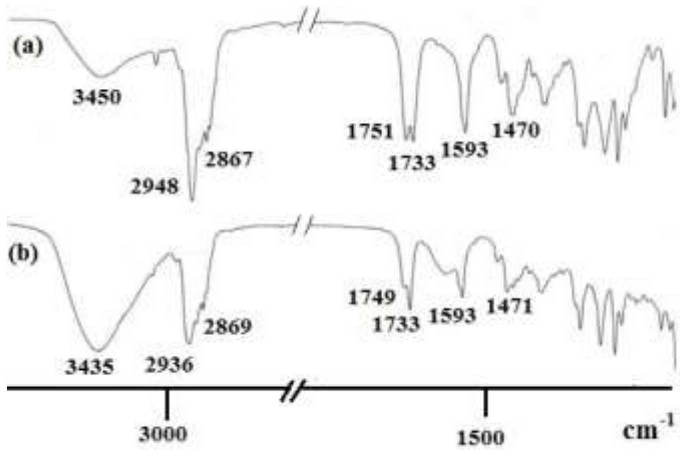

Fig. S1. Partial FTIR spectra of (a) **1** (amorphous) and (b) **1** in gel state.

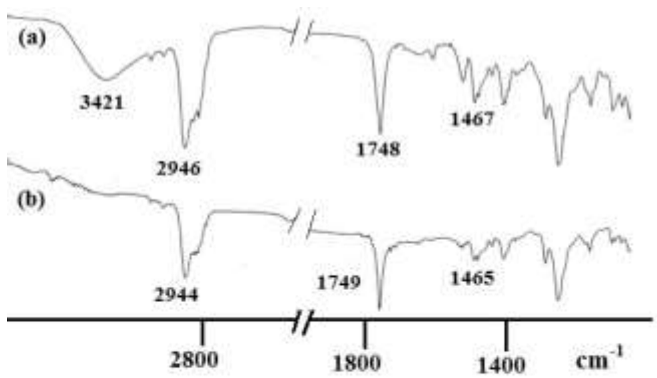

Fig. S2. Partial FTIR spectra of (a) **2** (amorphous) and (b) **2** in gel state.

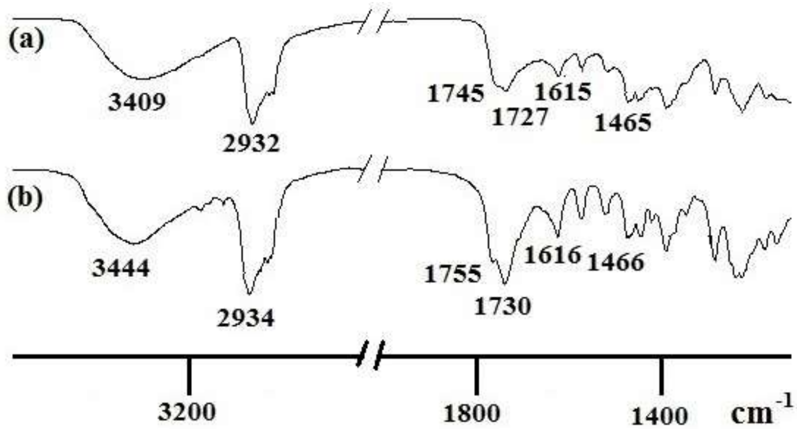

Fig. S3. Partial FTIR spectra of (a) **3** (amorphous) and (b) **3** in gel state.

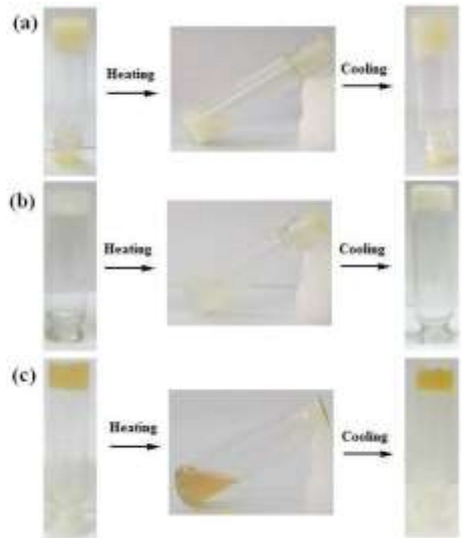

Fig. S4. Pictorial representation of the thermo reversibility of the $CHCl_3$:CH_3OH (2:1, v/v) gels of (a) **1**, (b) **2** and (c) **3**.

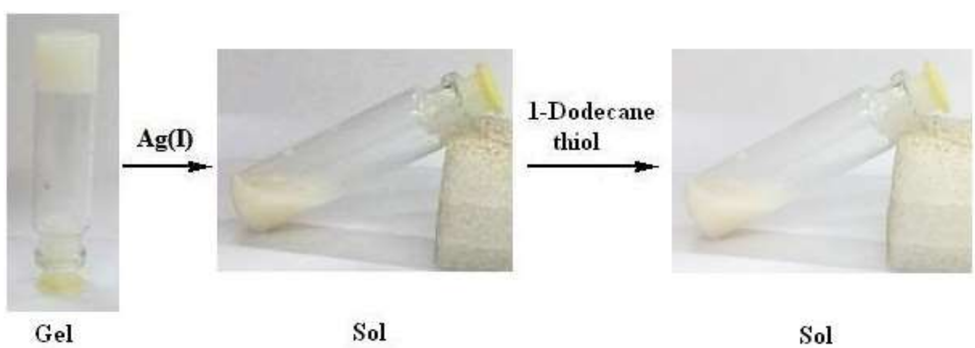

Fig. S5. Pictorial representation of Ag^+ (c = 0.2 M, 5 equiv.) induced broken gels of **2** [15 mg/ mL in $CHCl_3$: MeOH (2:1, v/v)] upon addition of 1-Dodecanethiol (in excess amounts) after 4h.

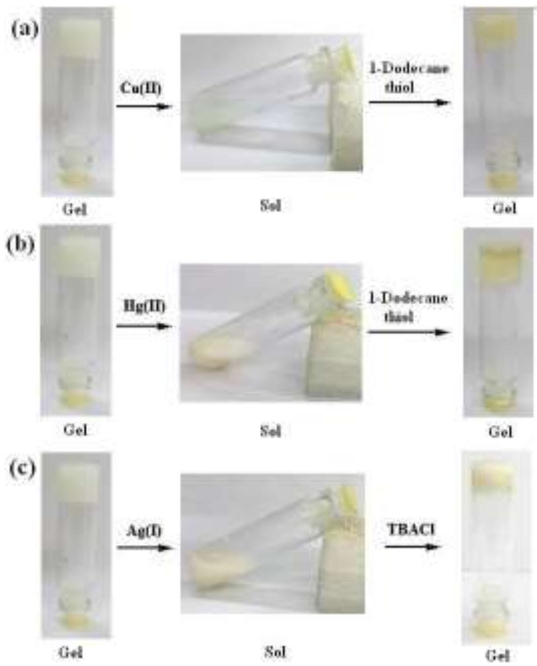

Fig. S6. Chemical responsiveness of the gel of **2** [15 mg/ mL in $CHCl_3$: MeOH (2:1, v/v)] on successive addition of (a) Cu^{2+} (c = 0.2 M, 5 equiv.) and 1-dodecanethiol (c = 0.2 M, 10 equiv); (b) Hg^{2+} (c = 0.2 M, 5 equiv.) and 1-dodecanethiol (c = 0.2 M, 10 equiv) and (c) Ag^{+} (c = 0.2 M, 5 equiv.) and TBACl (c = 0.2 M, 5 equiv).

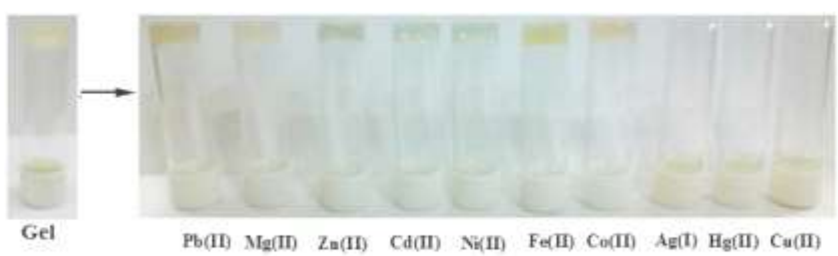

Fig. S7. Photograph showing the changes in the gel state of **3** (15 mg/ mL) when the gels were prepared with 5 equiv. amounts of different metal ions [c = 0.2 M in $CHCl_3$:CH_3OH (2:1, v/v) as perchlorate salt] in $CHCl_3$:CH_3OH (2:1, v/v). Similar observation was obtained when the $CHCl_3$:CH_3OH (2:1, v/v) gels of **3** were kept in contact with 0.5 mL of different metal solution [c = 0.2 M in $CHCl_3$:CH_3OH (2:1, v/v)].

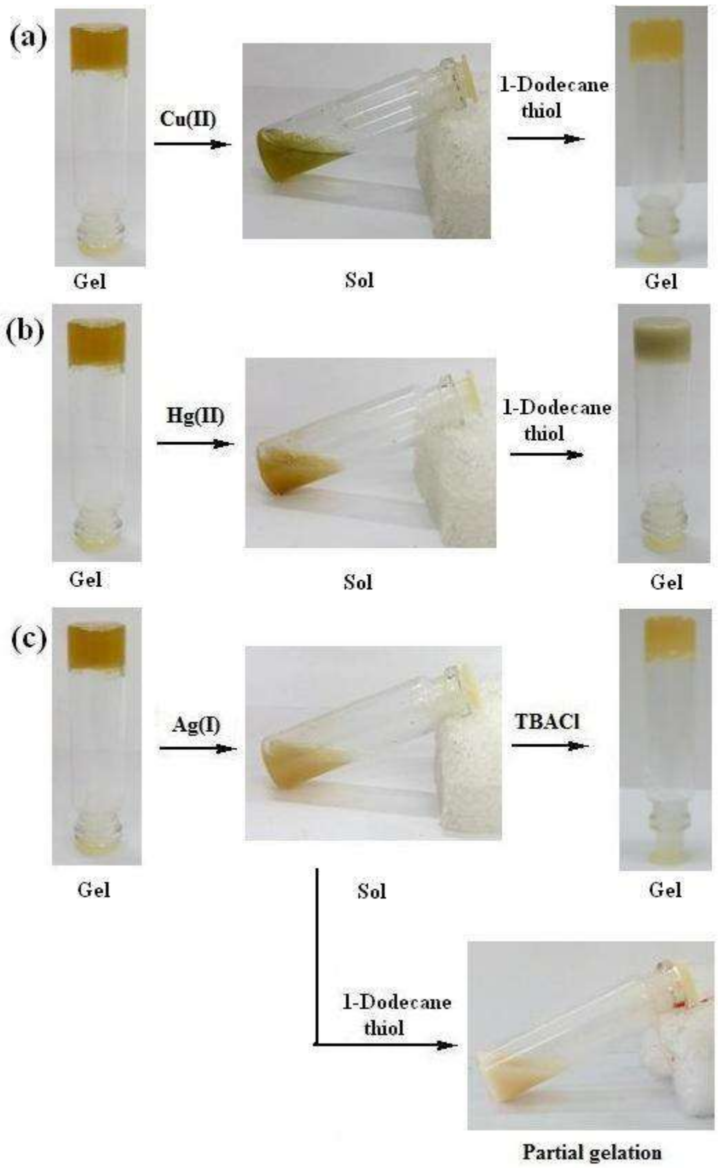

Fig. S8. Chemical responsiveness of the gel of **3** [15 mg/ mL in $CHCl_3$: MeOH (2:1, v/v)] on successive addition of (a) Cu^{2+} (c = 0.2 M, 5 equiv.) and 1-dodecanethiol (c = 0.2 M, 10 equiv); (b) Hg^{2+} (c = 0.2 M, 5 equiv.) and 1-dodecanethiol (c = 0.2 M, 10 equiv) and (c) Ag^{+} (c = 0.2 M, 5 equiv.) and TBACl (c = 0.2 M, 5 equiv) and 1-dodecanethiol (in excess amounts).

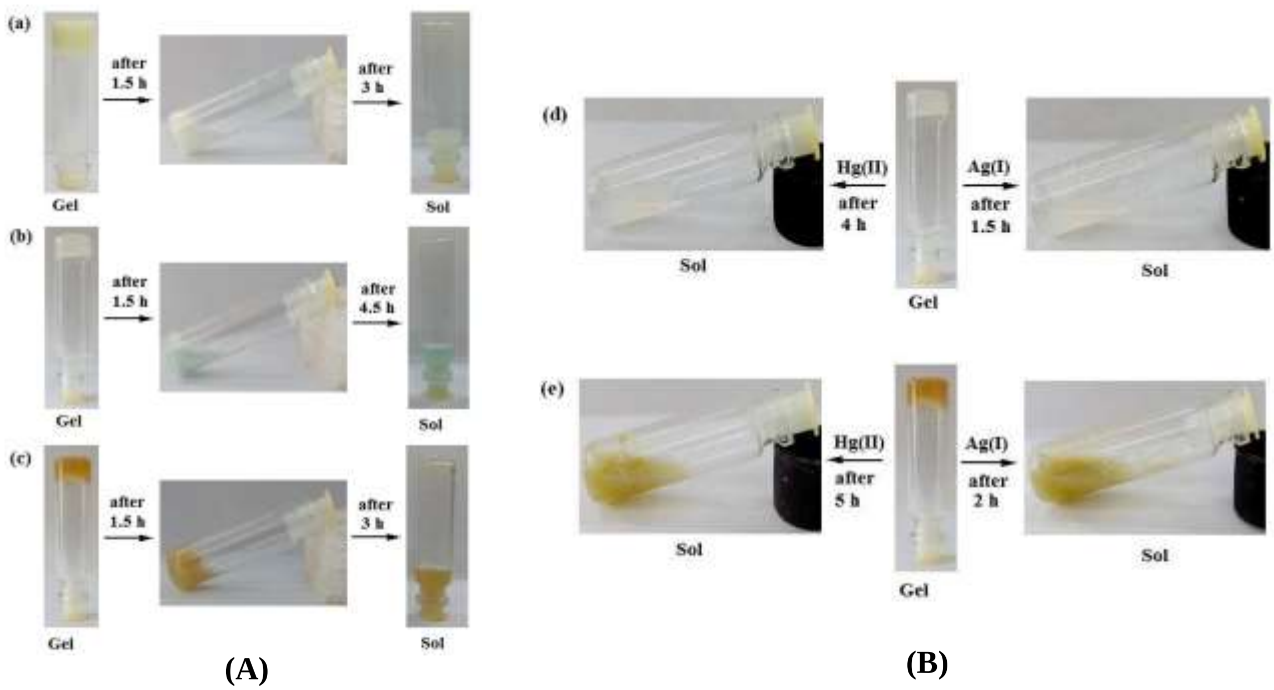

Fig. S9. (A) Pictorial representations of the phase changes of the gels of (a) **1**; (b) **2** and (c) **3** [15 mg/ mL in $CHCl_3$: MeOH (2:1, v/v)] in presence of 1 equiv. amounts of Cu^{2+} (c = 0.2 M) with time. (B) Pictorial representations of the phase changes of the gels of (d) **2** and (e) **3** [15 mg/ mL in $CHCl_3$: MeOH (2:1, v/v)] in presence of 1 equiv. amount of respective metal ions (c = 0.2 M) with time.

Change in emission of 3 in CH_3CN: $CHCl_3$ (4:1, v/v).

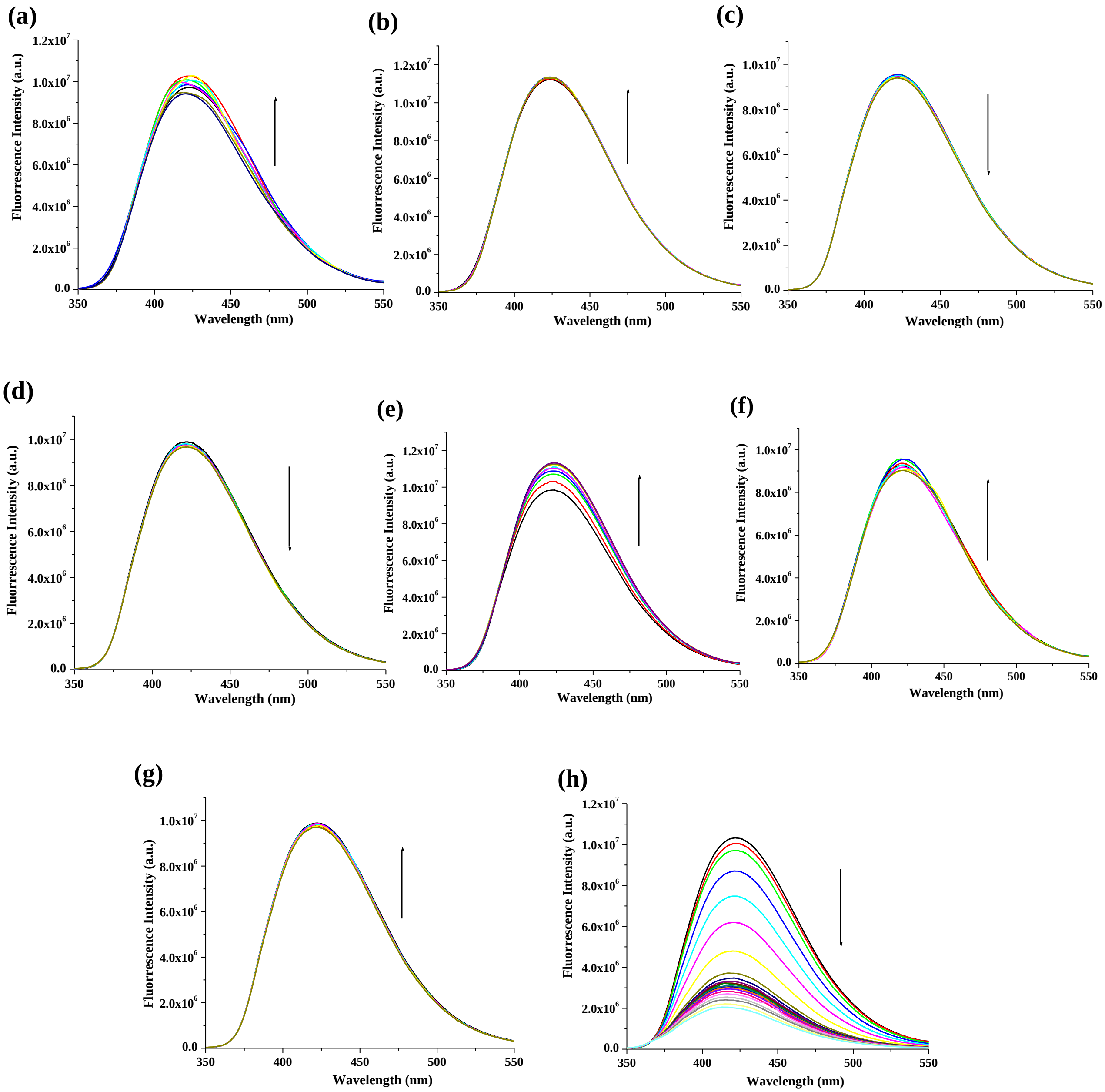

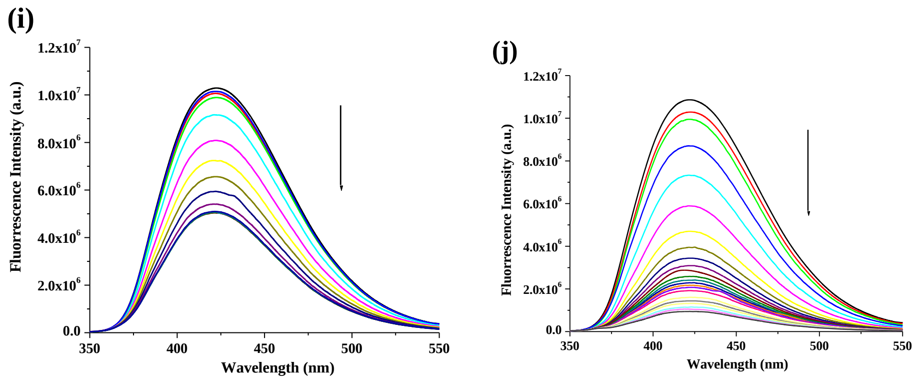

Fig. S10. Change in emission of **3** ($c = 2.0 \times 10^{-5}$ M) upon addition of 5 equiv. amount of (a) Pb^{2+}, (b) Mg^{2+}, (c) Co^{2+}, (d) Ni^{2+}, (e) Zn^{2+}, (f) Cd^{2+}, (g) Fe^{2+}, (h) Hg^{2+}, (i) Ag^{+}, (j) Cu^{2+} ($c = 8.0 \times 10^{-4}$ M) in CH_3CN: $CHCl_3$ (4:1, v/v).

Job plot

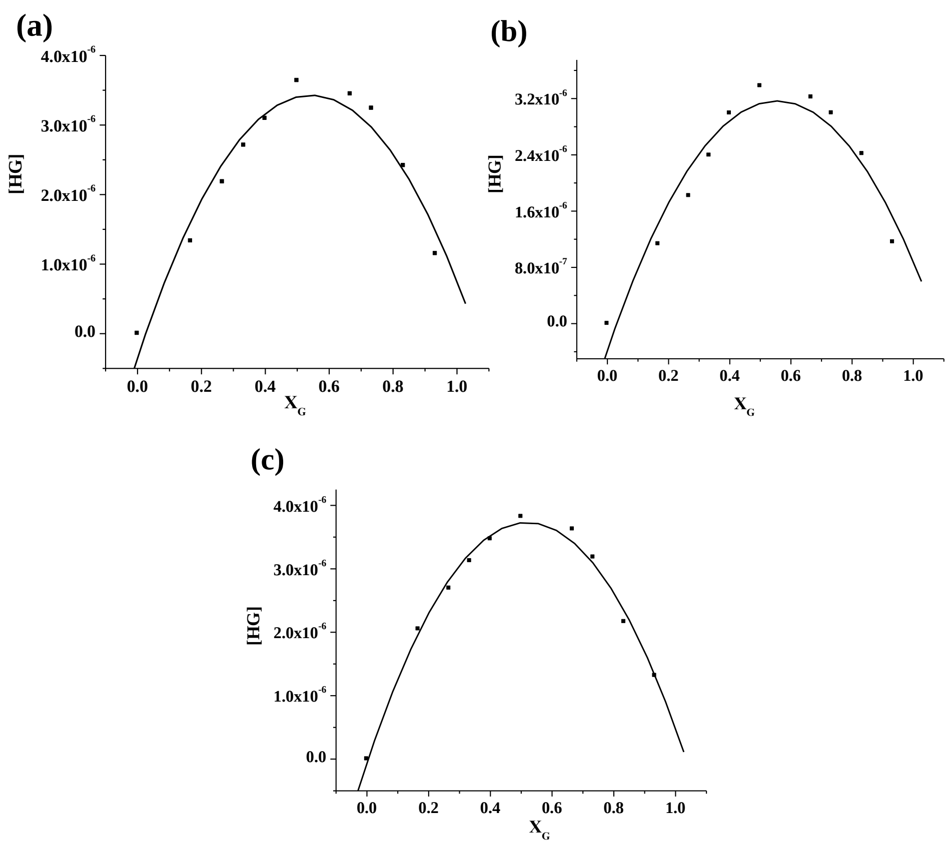

Fig. S11. Job plot of receptor **3** ($c = 2.0 \times 10^{-5}$ M) with (a) Hg^{2+}, (b) Ag^{+} and (c) Cu^{2+} from fluorescence.

Job plot

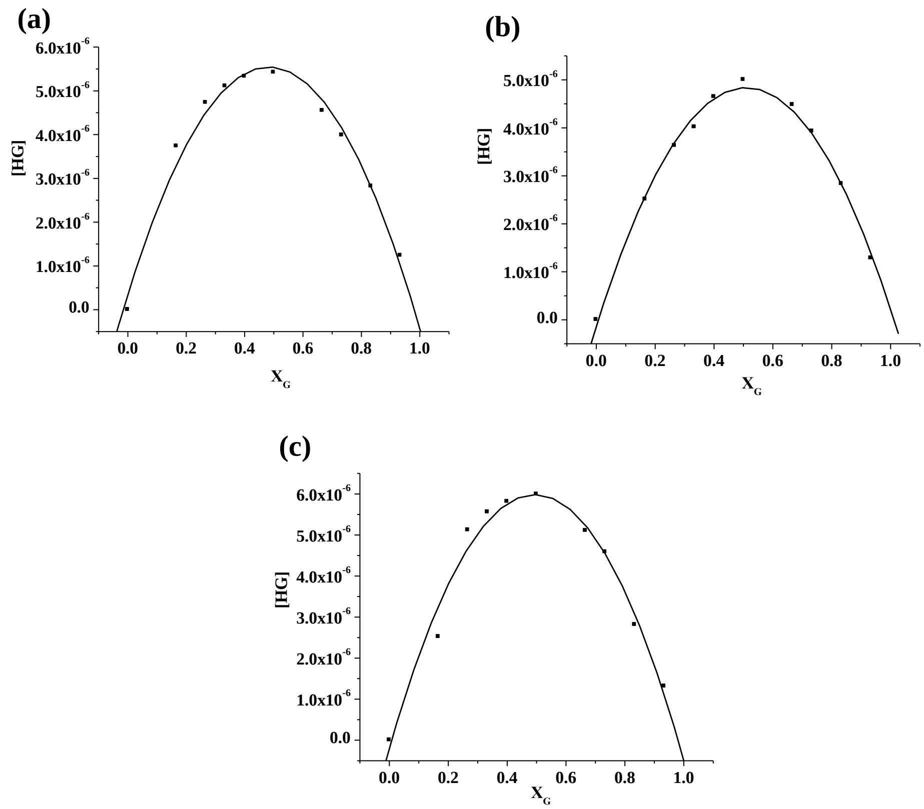

Fig. S12. Job plot of receptor **3** (c = 2.0 x 10^{-5} M) with (a) Hg^{2+}, (b) Ag^{+} and (c) Cu^{2+} from UV.

Change in absorbance of 3 in CH_3CN: $CHCl_3$ (4:1, v/v).

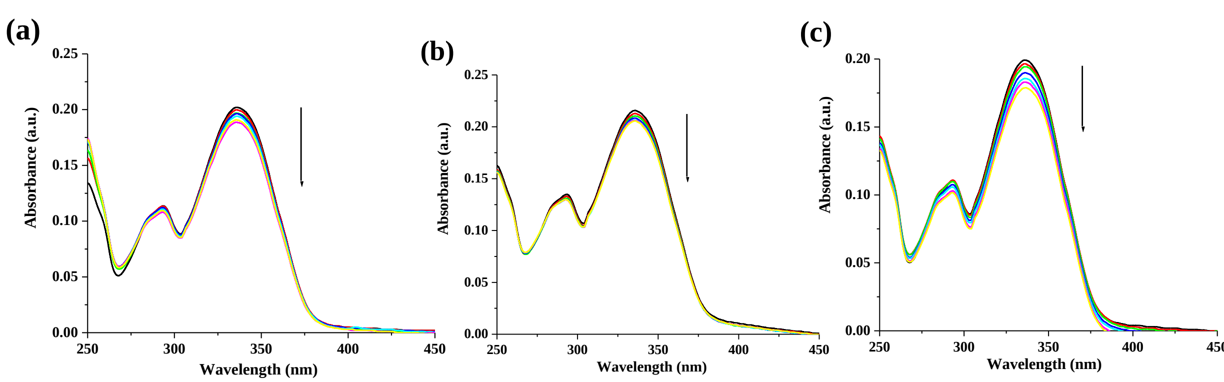

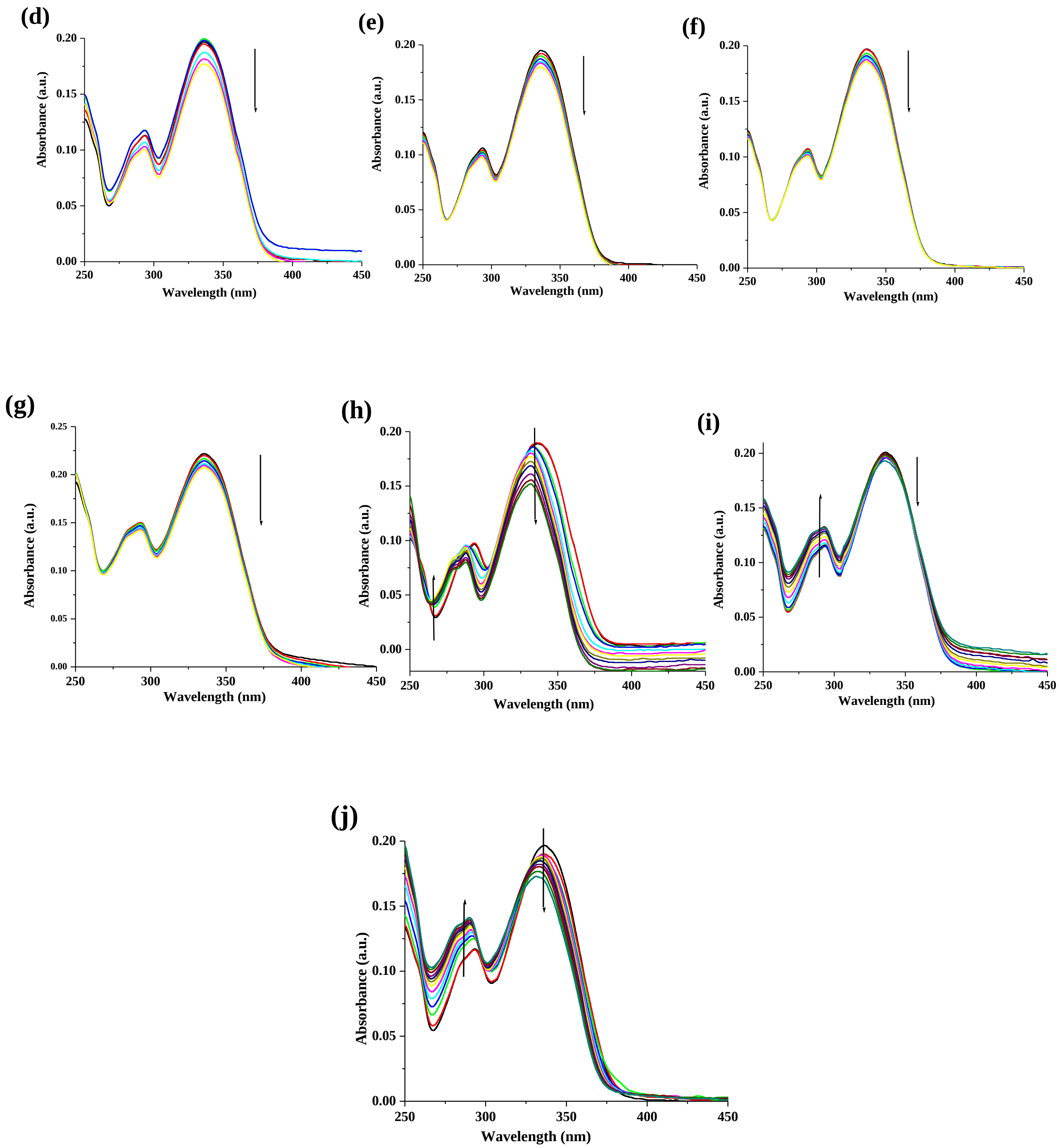

Fig. S13. Change in absorbance of **3** (c = 2.0 x 10^{-5} M) upon addition of 5 equiv. amount of (a) Pb^{2+}, (b) Mg^{2+}, (c) Co^{2+}, (d) Ni^{2+}, (e) Zn^{2+}, (f) Cd^{2+}, (g) Fe^{2+}, (h) Hg^{2+}, (i) Ag^{+}, (j) Cu^{2+} (c = 8.0 x 10^{-4} M) in CH_3CN: $CHCl_3$ (4:1, v/v).

Change in absorbance of 1 in CH_3CN: $CHCl_3$ (4:1, v/v)

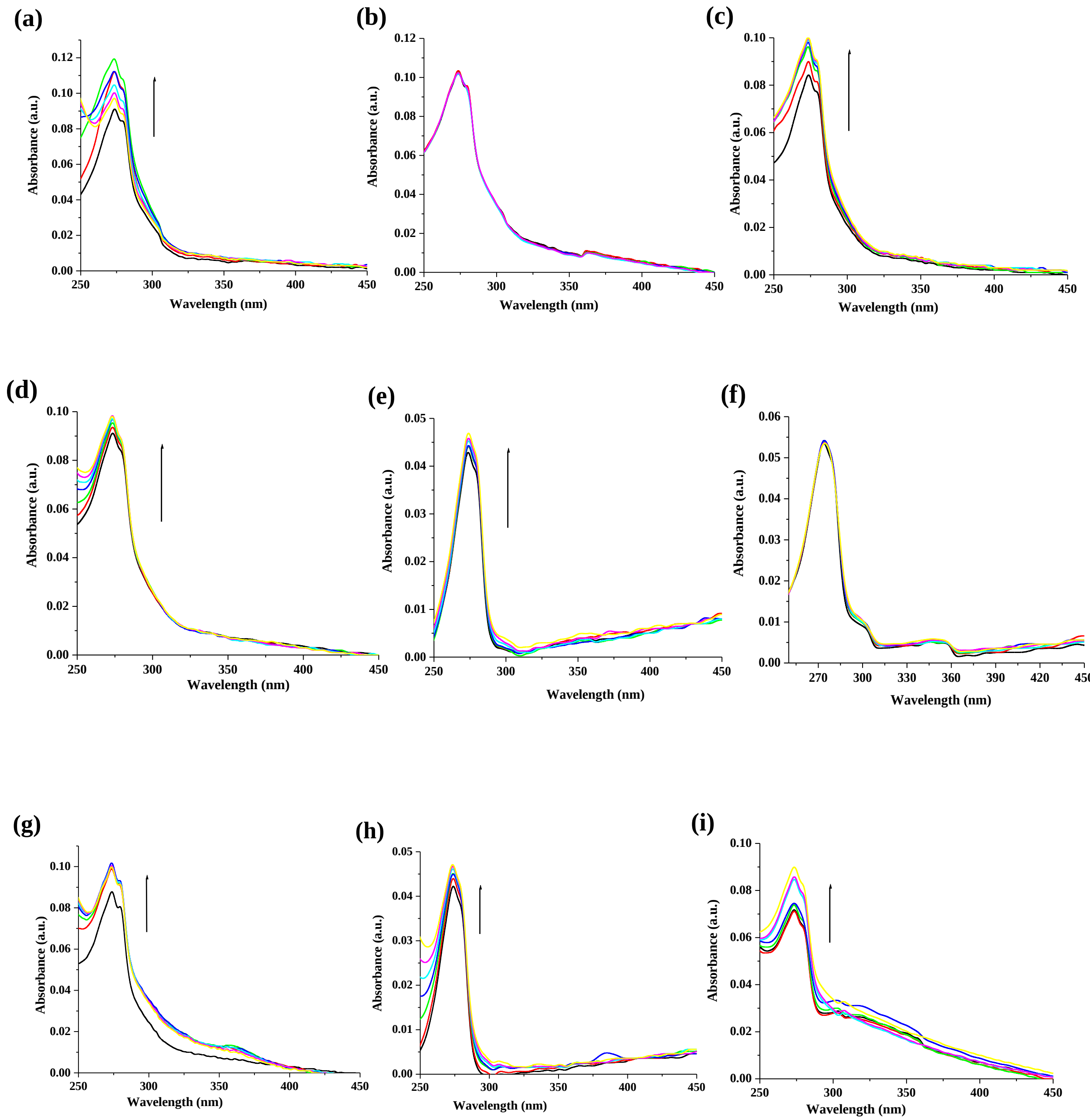

(j)

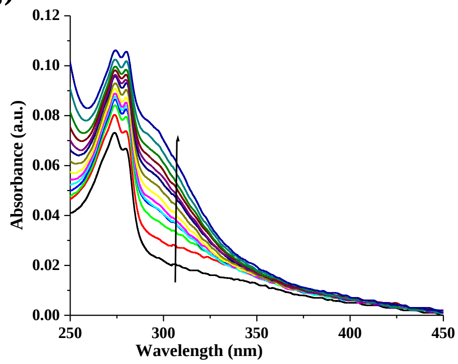

Fig. S14. Change in absorbance of **1** (c = 2.0 x 10^{-5} M) upon addition of 5 equiv. amount of (a) Pb^{2+}, (b) Mg^{2+}, (c) Co^{2+}, (d) Ni^{2+}, (e) Zn^{2+}, (f) Cd^{2+}, (g) Fe^{2+}, (h) Hg^{2+}, (i) Ag^{+}, (j) Cu^{2+} (c = 8.0 x 10^{-4} M) in CH_3CN: $CHCl_3$ (4:1, v/v).

Change in absorbance of 2 in CH_3CN: $CHCl_3$ (4:1, v/v)

(a)

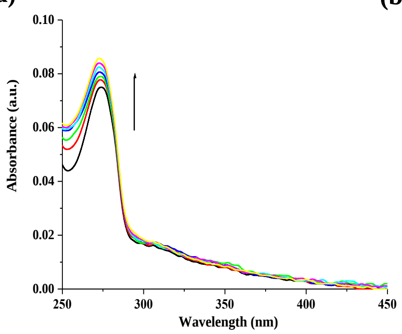

(b)

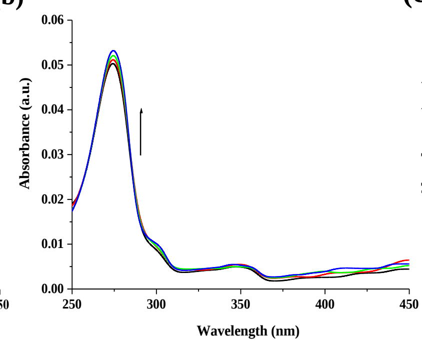

(c)

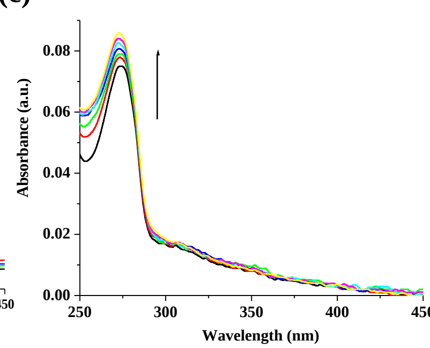

(d)

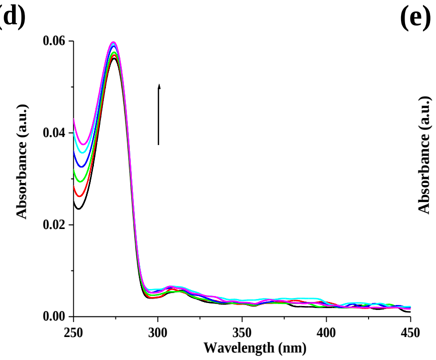

(e)

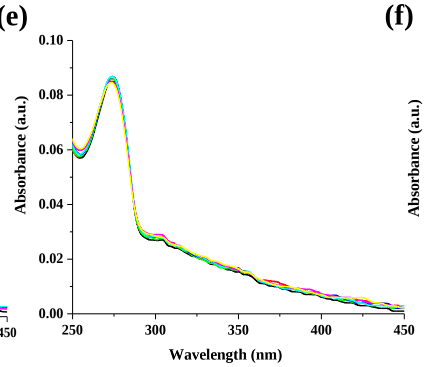

(f)

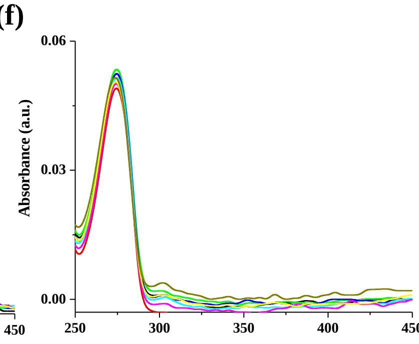

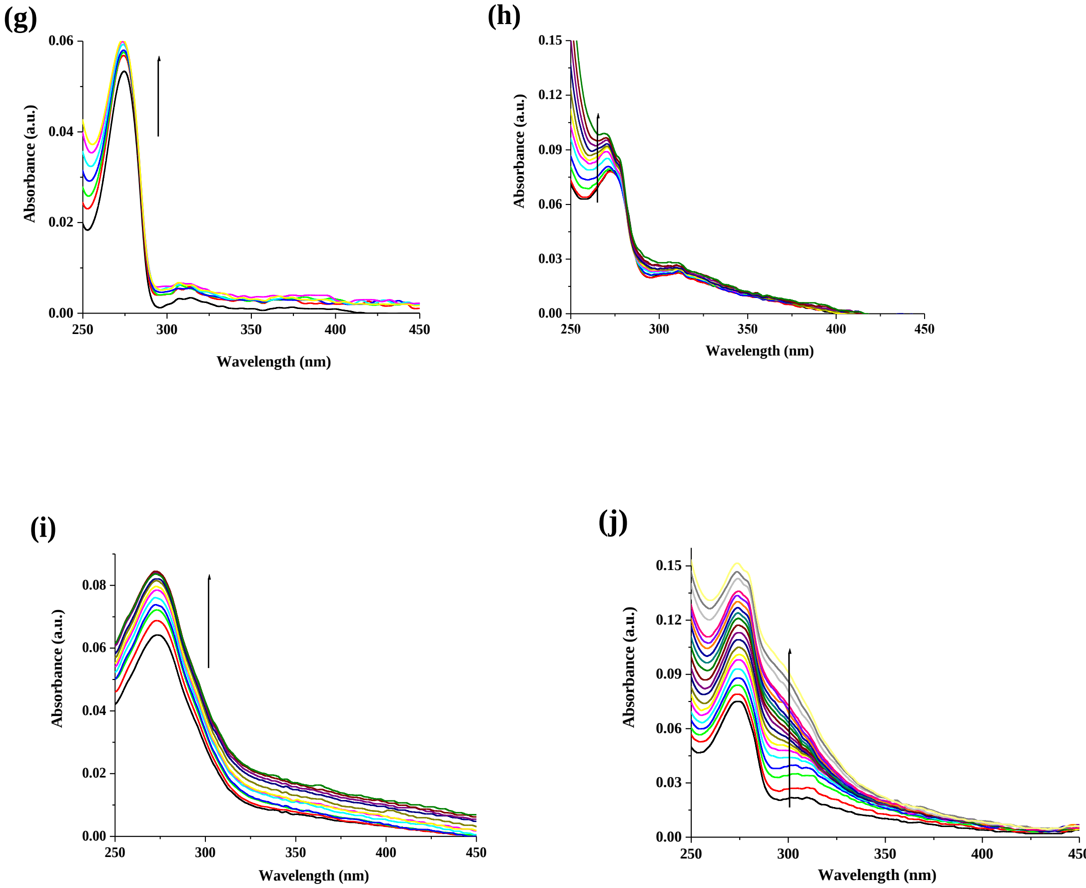

Fig. S15. Change in absorbance of **2** (c = 2.0 x 10^{-5} M) upon addition of 5 equiv. amount of (a) Pb^{2+}, (b) Mg^{2+}, (c) Co^{2+}, (d) Ni^{2+}, (e) Zn^{2+}, (f) Cd^{2+}, (g) Fe^{2+}, (h) Hg^{2+}, (i) Ag^{+}, (j) Cu^{2+} (c = 8.0 x 10^{-4} M) in CH_3CN: $CHCl_3$ (4:1, v/v).

Non liner binding constant curve from fluorescence

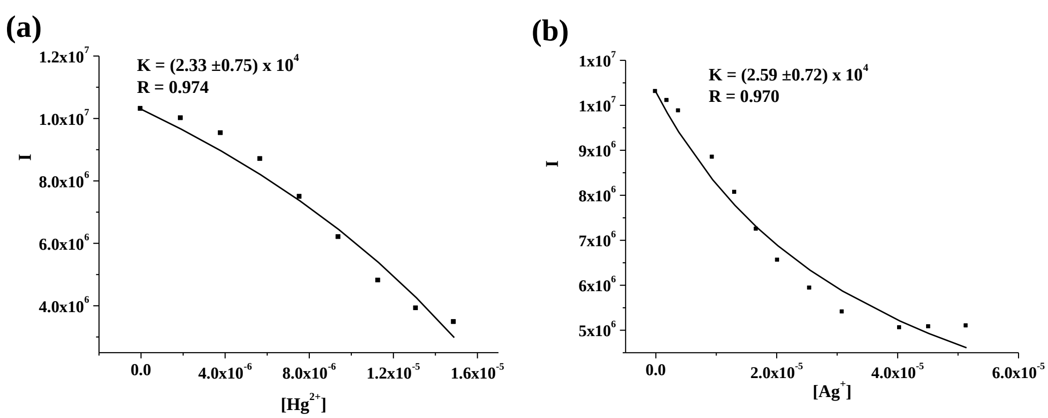

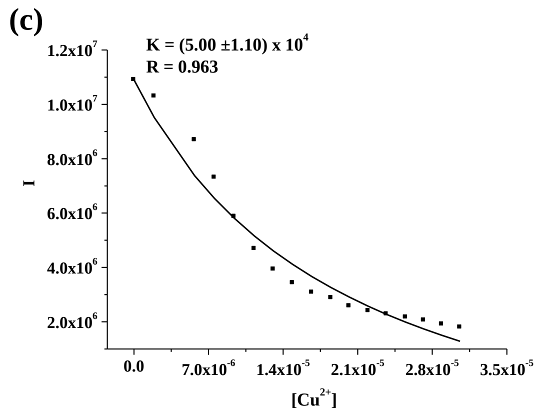

Fig. S16. Non liner binding constant curve for **3** (c = 2.0 x 10^{-5} M) with (a) Hg^{2+}, (b) Ag^{+} and (c) Cu^{2+} (c = 8.0 x 10^{-4} M) in CH_3CN: $CHCl_3$ (4:1, v/v) from fluorescence.

Non liner binding constant curve from UV

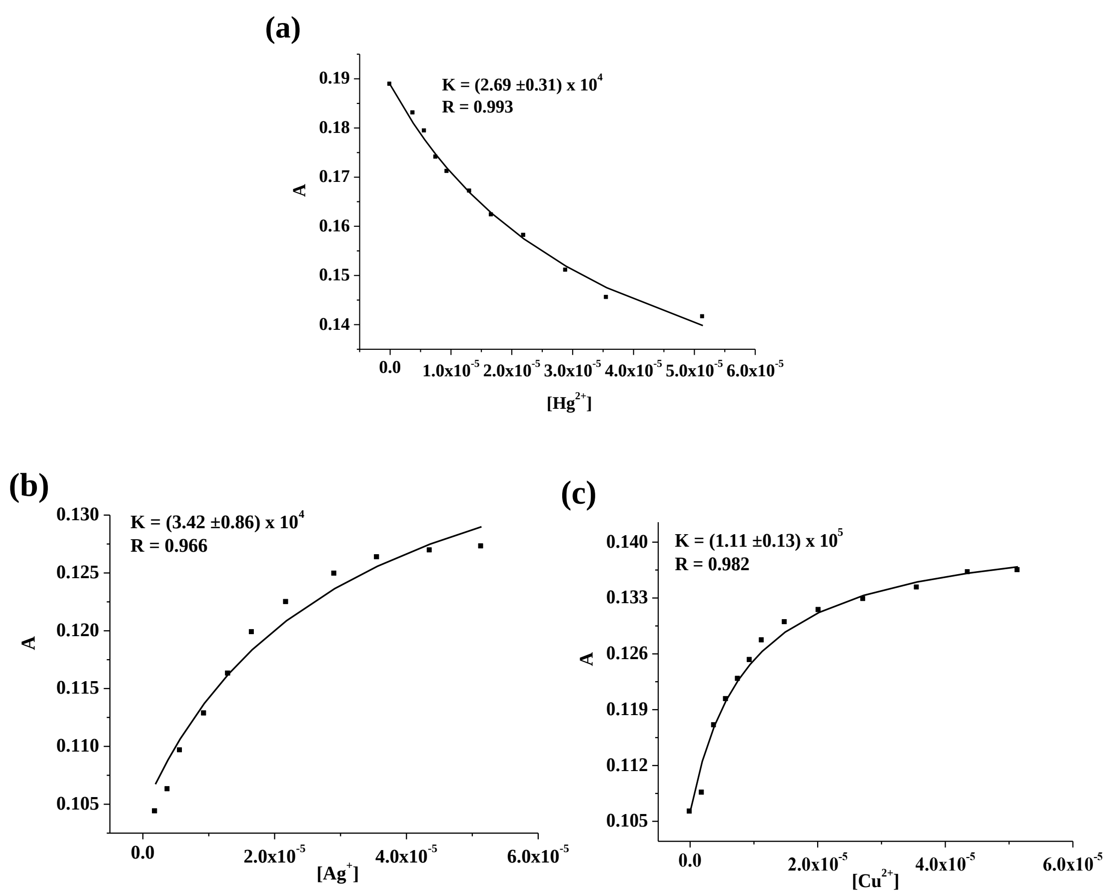

Fig. S17. Non liner binding constant curve for **3** (c = 2.0 x 10^{-5} M) with (a) Hg^{2+}, (b) Ag^{+} and (c) Cu^{2+} (c = 8.0 x 10^{-4} M) in CH_3CN: $CHCl_3$ (4:1, v/v) from UV.

Job plot

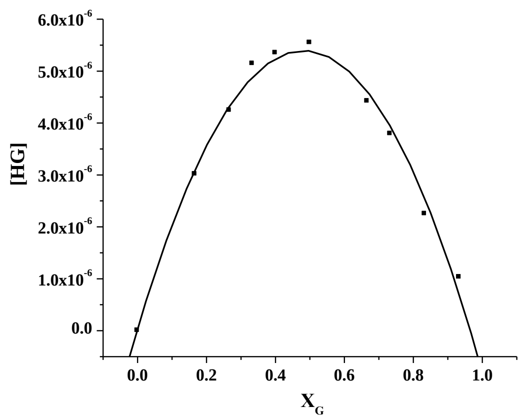

Fig. S18. Job plot of receptor **1** (c = 2.0 x 10^{-5} M) with Cu^{2+} from UV.

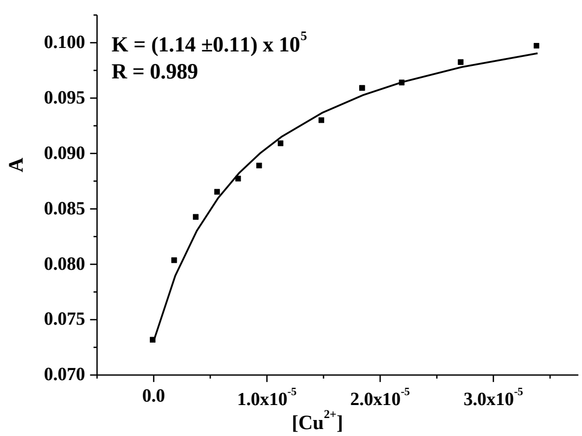

Fig. S19. Non liner binding constant curve for **1** (c = 2.0 x 10^{-5} M) with Cu^{2+} (c = 8.0 x 10^{-4} M) in CH_3CN: $CHCl_3$ (4:1, v/v) from UV.

Job plot

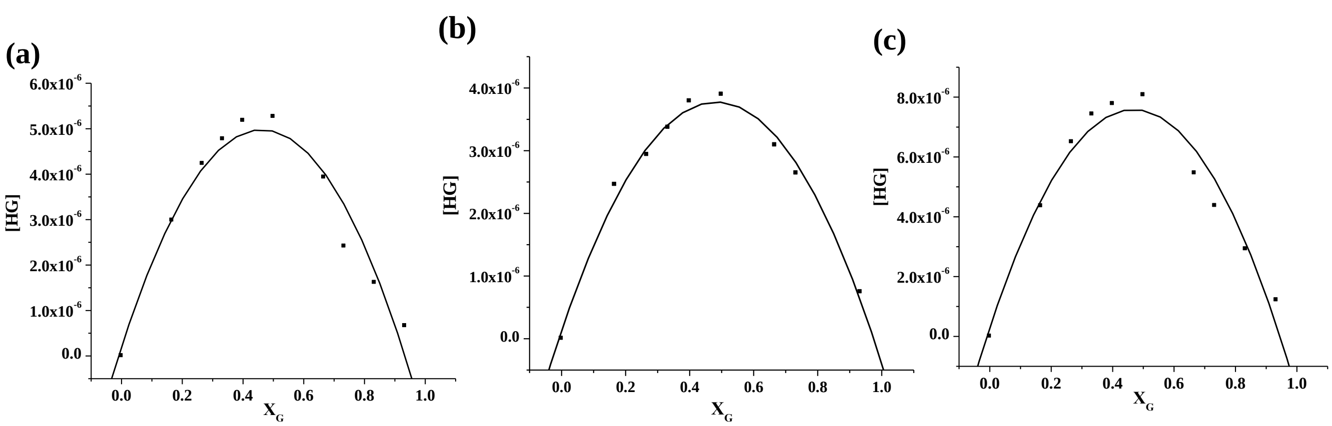

Fig. S20. Job plot of receptor **2** (c = 2.0 x 10^{-5} M) with (a) Hg^{2+}, (b) Ag^{+} and (c) Cu^{2+} from UV.

Non liner binding constant curve

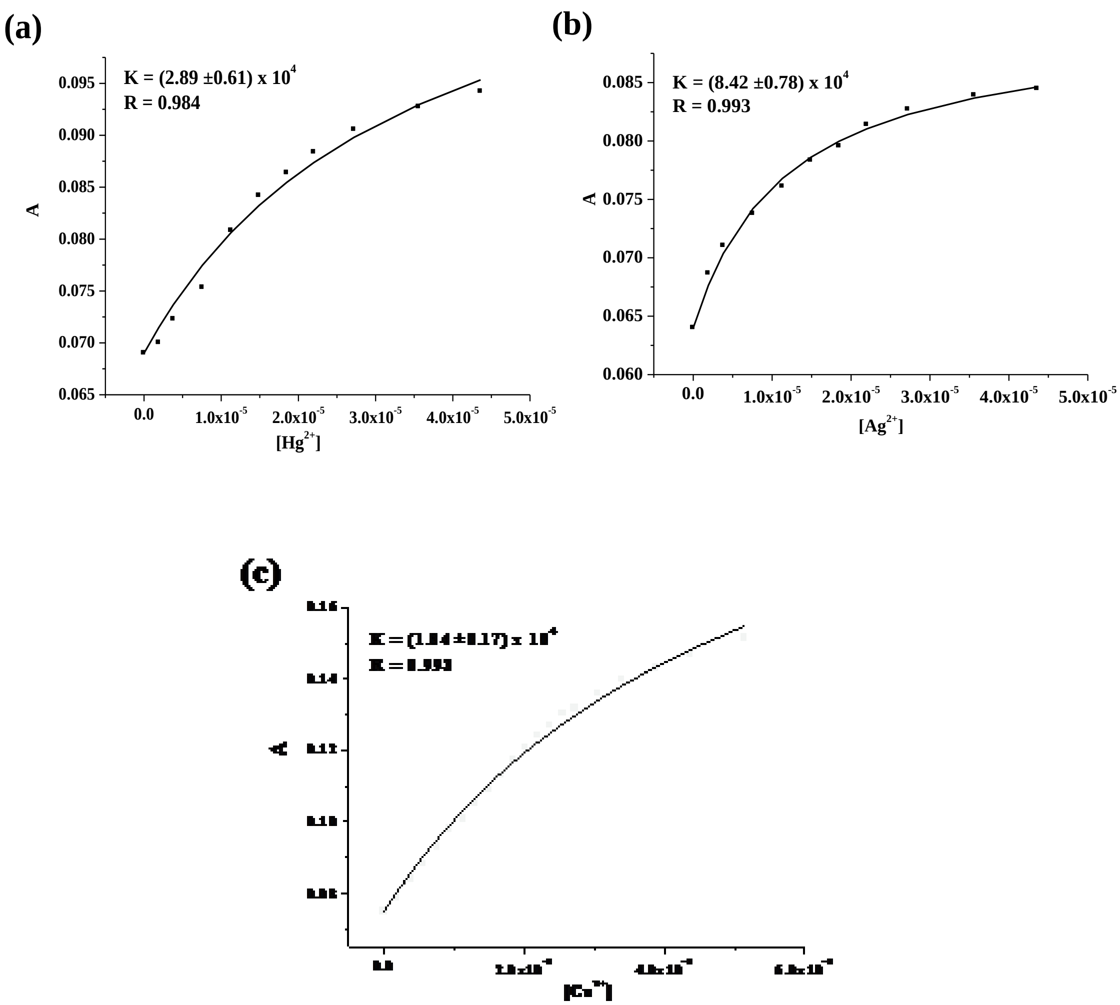

Fig. S21. Non liner binding constant curve for **2** (*c* = 2.0 x 10^{-5} M) with (a) Hg^{2+}, (b) Ag^{+} and (c) Cu^{2+} (*c* = 8.0 x 10^{-4} M) in CH_3CN: $CHCl_3$ (4:1, v/v) from UV.

^{1}H NMR change with metal ions

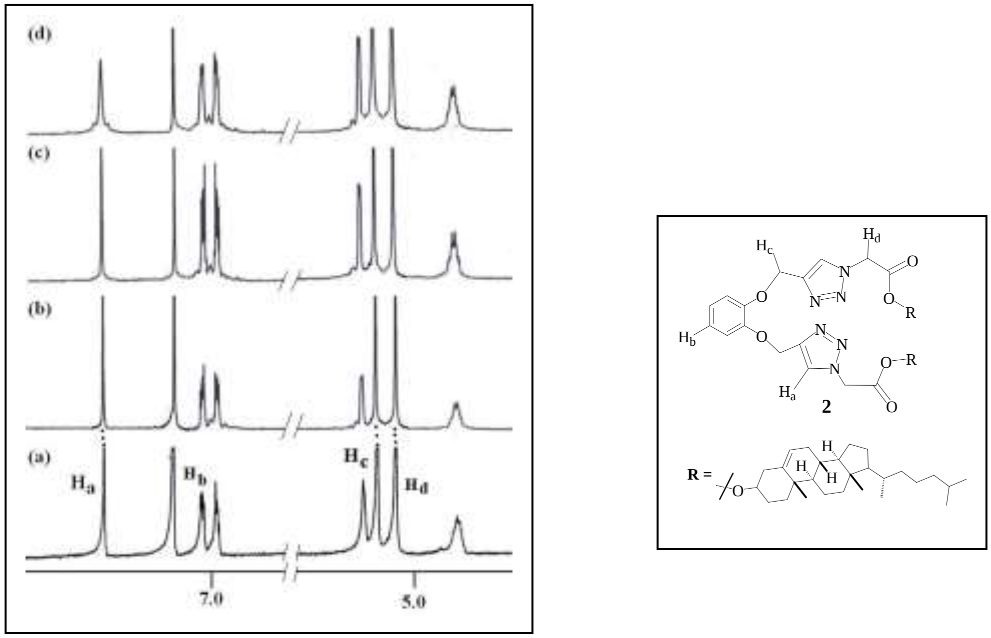

Fig. S22. Partial ^{1}H NMR (400 MHz, $CDCl_3$) of (a) compound **2** (c = 6.18 x 10^{-3} M),(b) **2** with Ag^{+} (1:1), (c) **2** with Hg^{2+} (1:1) and (d) **2** with Cu^{2+} (1:1).

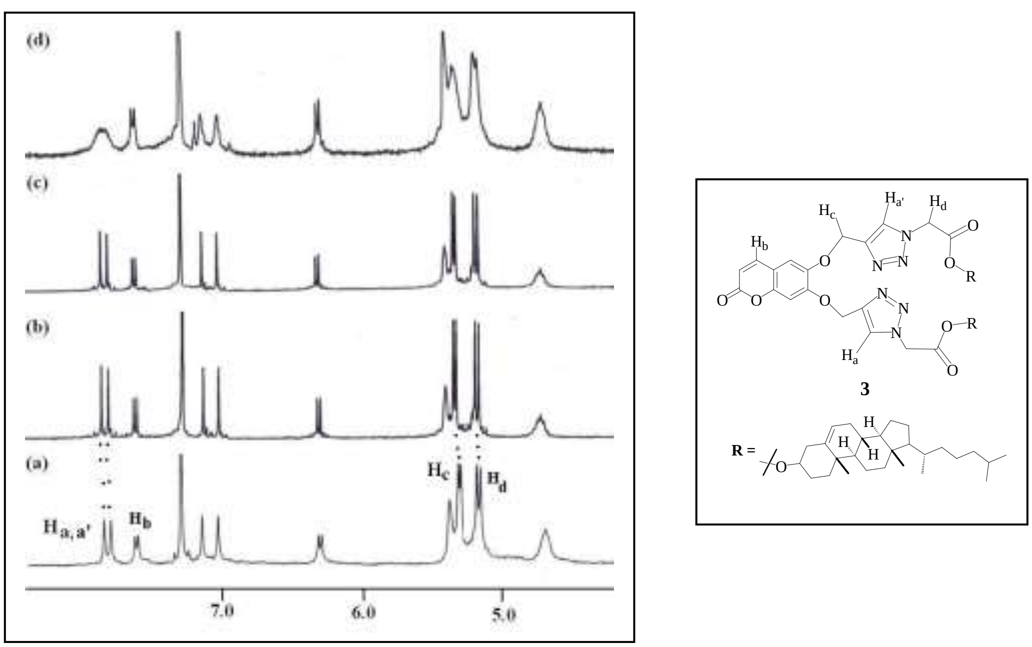

Fig. S23. Partial ^{1}H NMR (400 MHz, $CDCl_3$) of (a) compound **3** (c = 4.10 x 10^{-3} M),(b) **3** with Ag^{+} (1:1), (c) **3** with Hg^{2+} (1:1) and (d) **3** with Cu^{2+} (1:1).

^{1}H NMR ($CDCl_3$, 400 MHz)

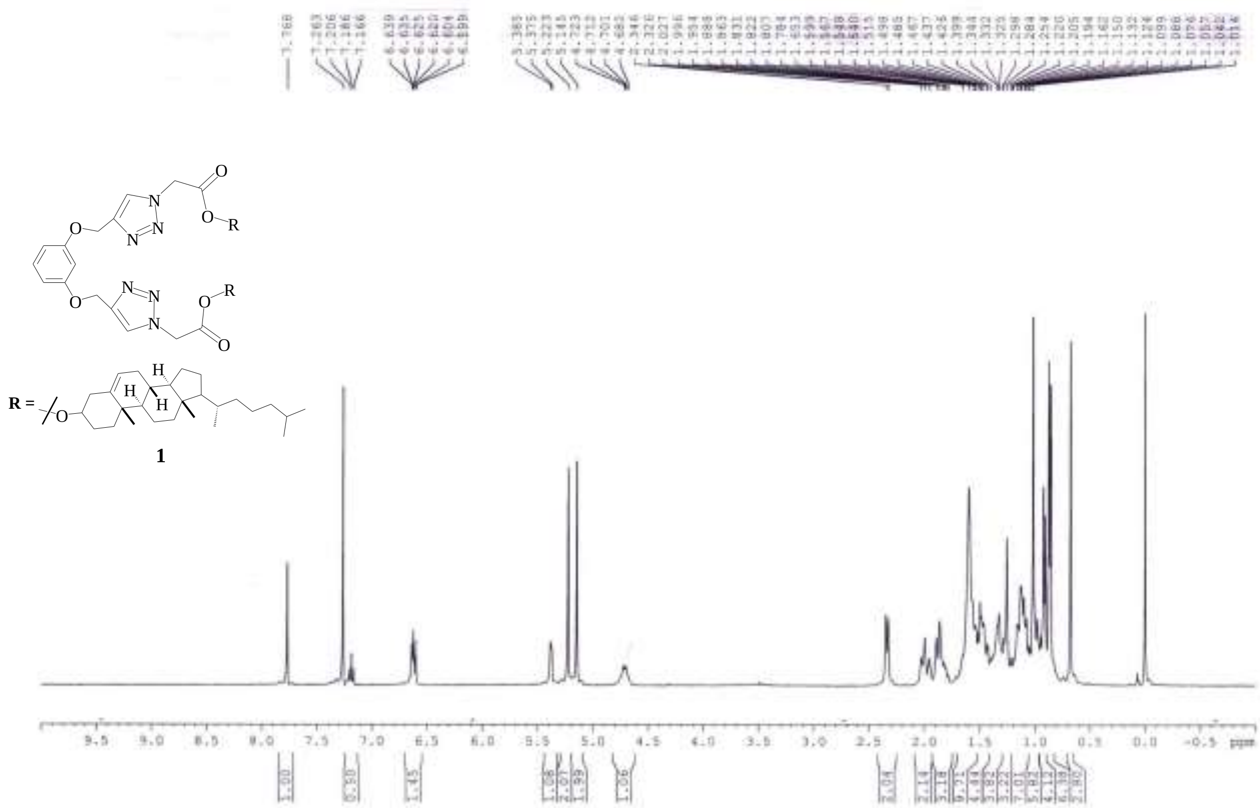

1

^{13}C NMR ($CDCl_3$, 100 MHz)

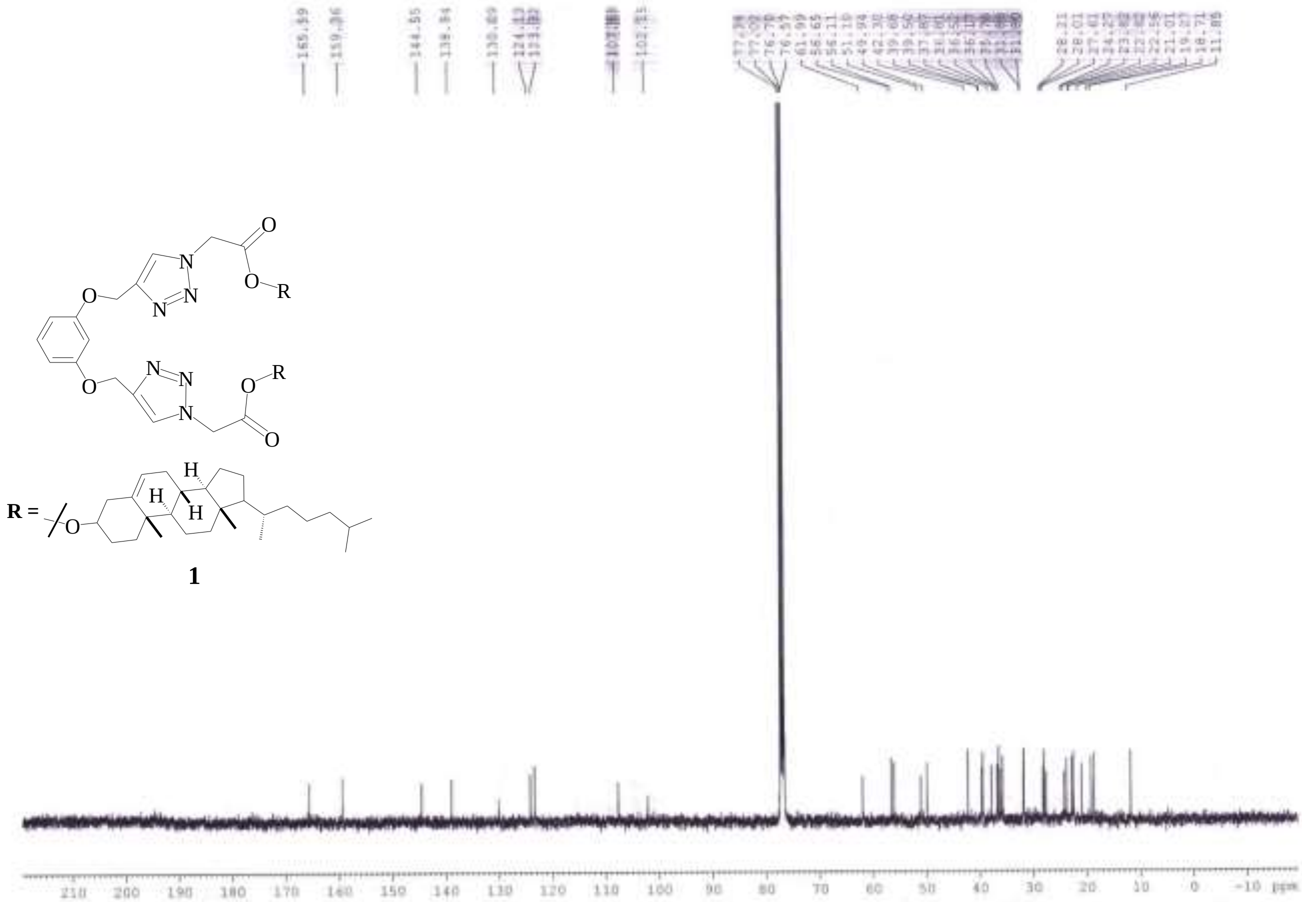

Mass spectrum of 1.

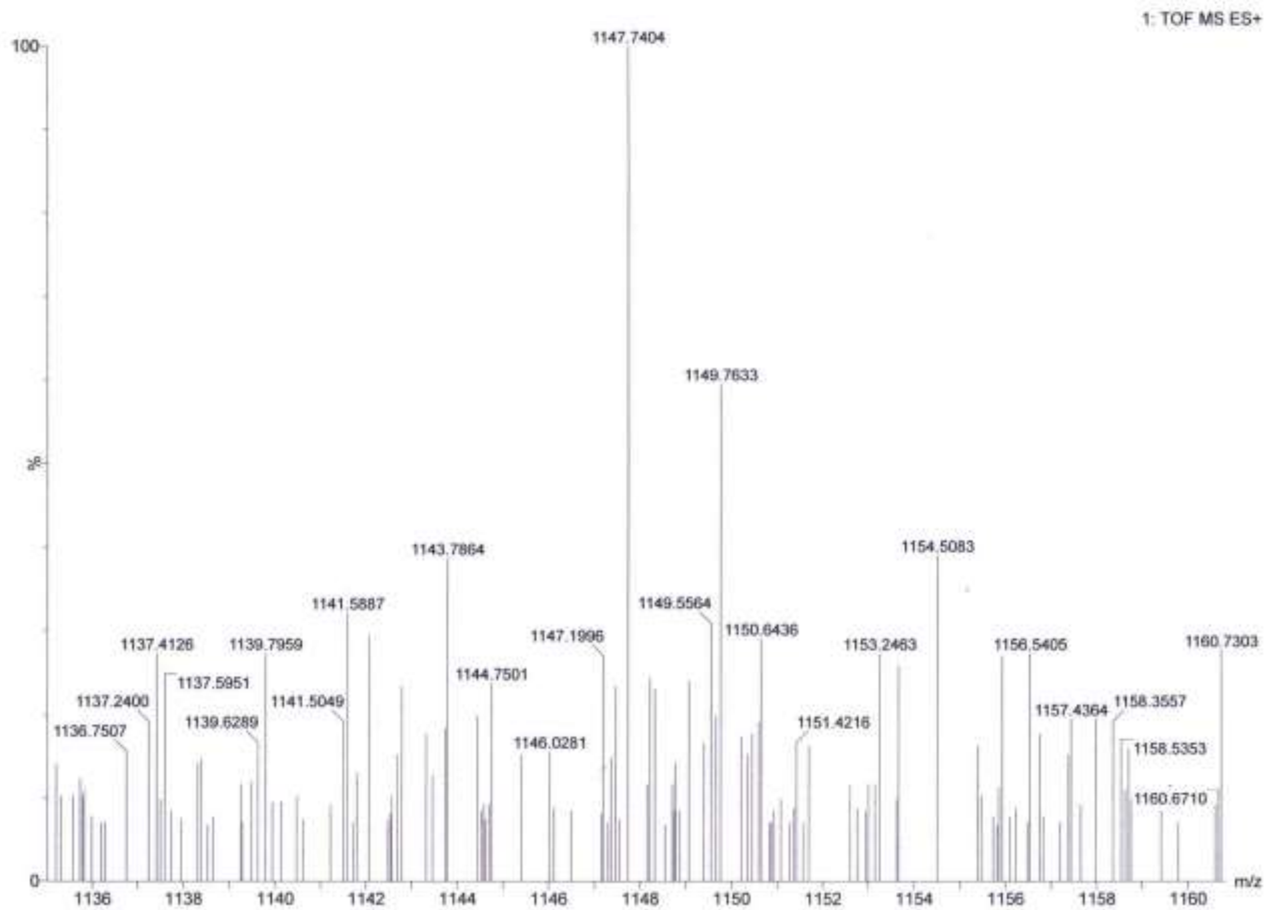

^{1}H NMR ($CDCl_3$, 400 MHz)

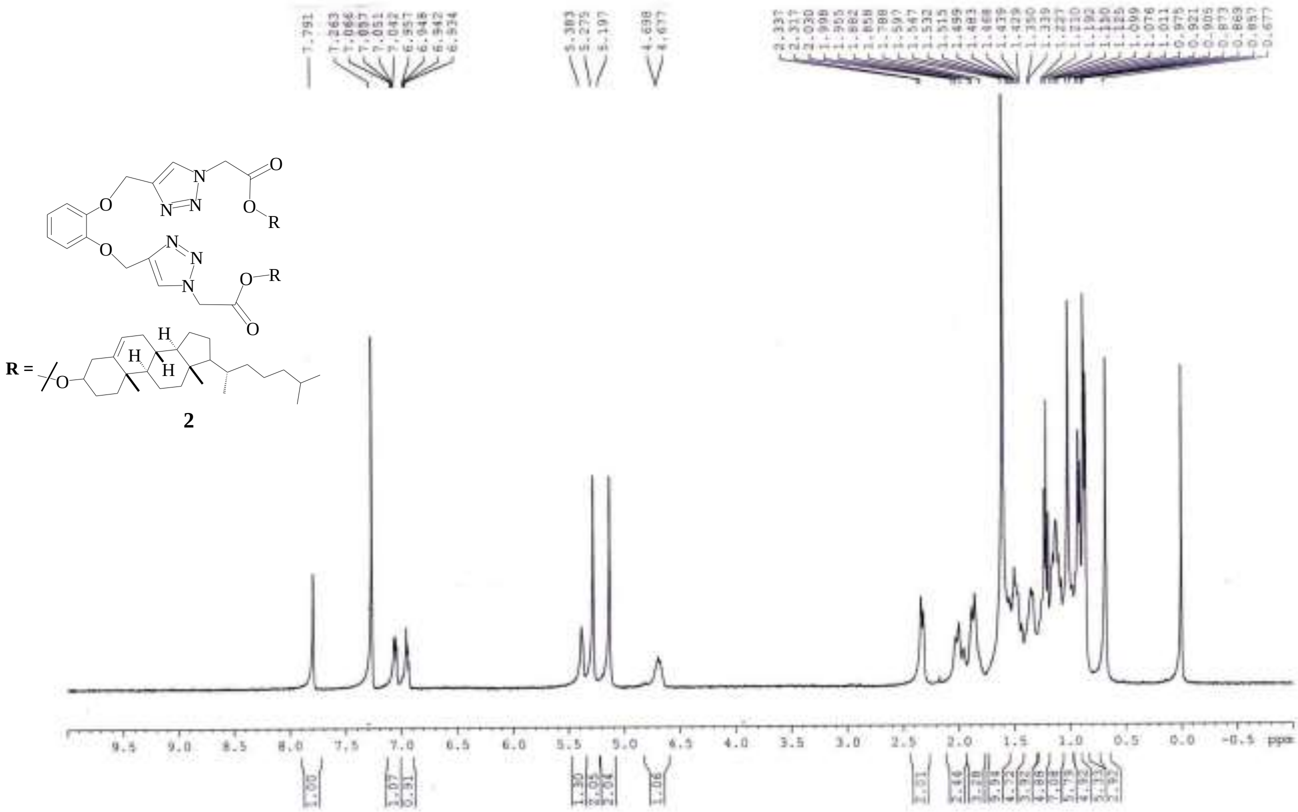

^{13}C NMR ($CDCl_3$, 100 MHz)

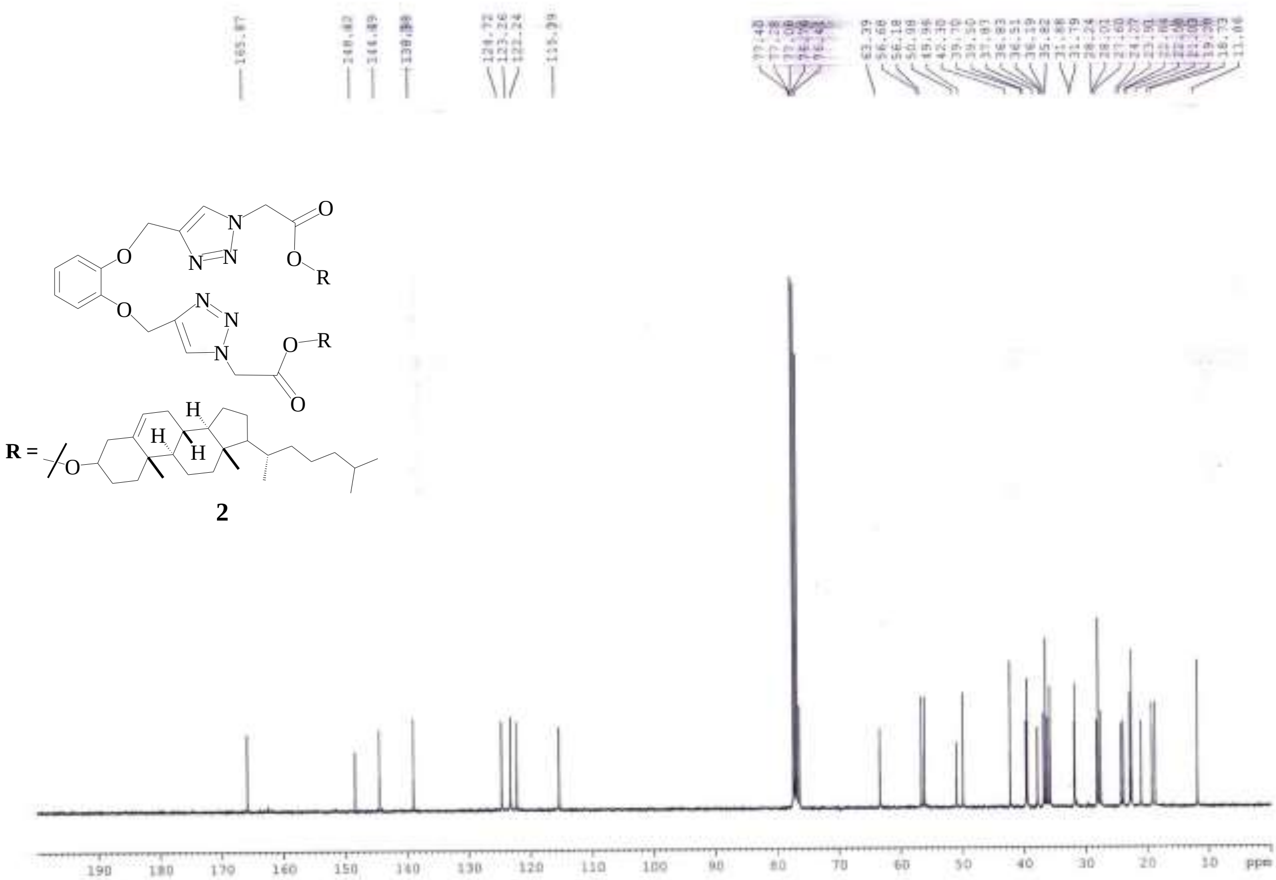

2

Mass spectrum of 2.

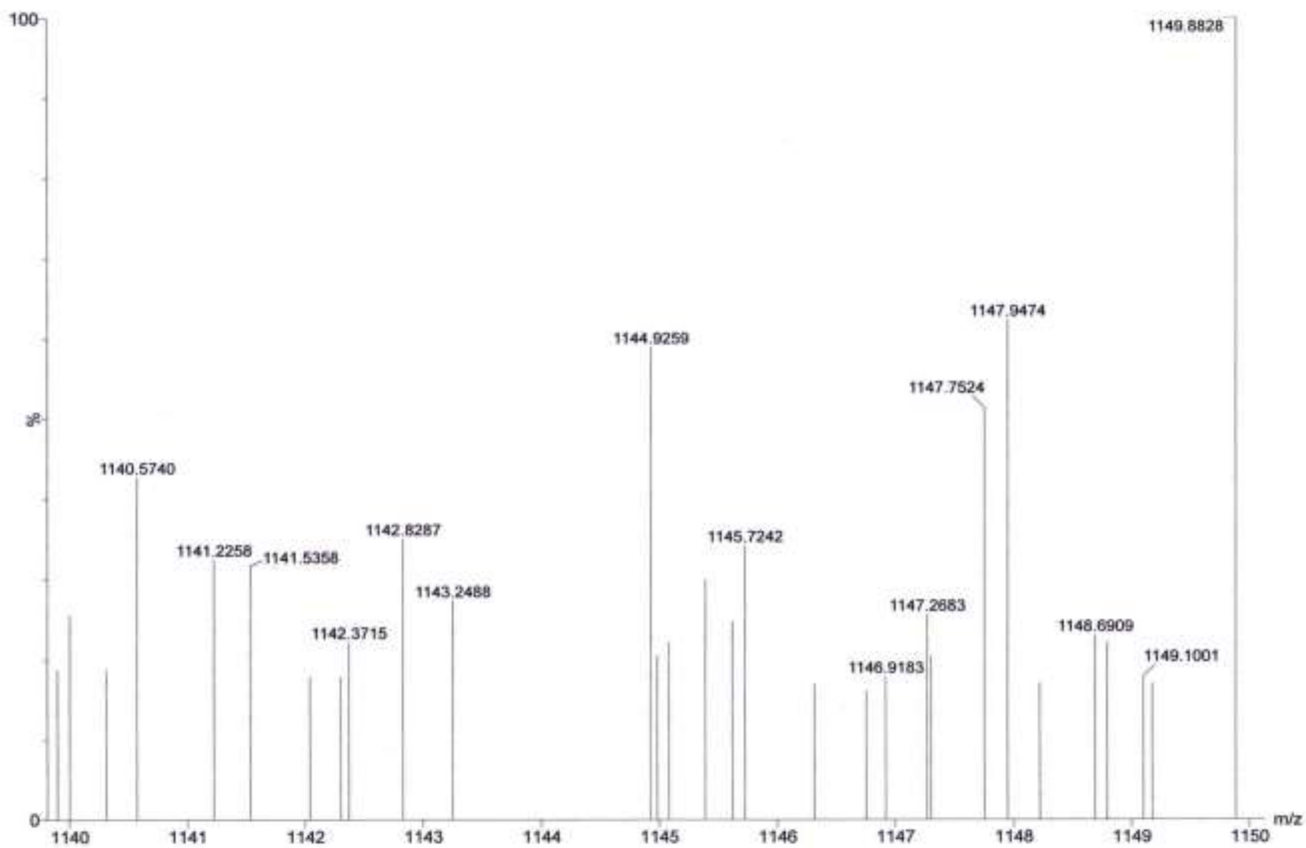

^{1}H NMR ($CDCl_3$, 400 MHz)

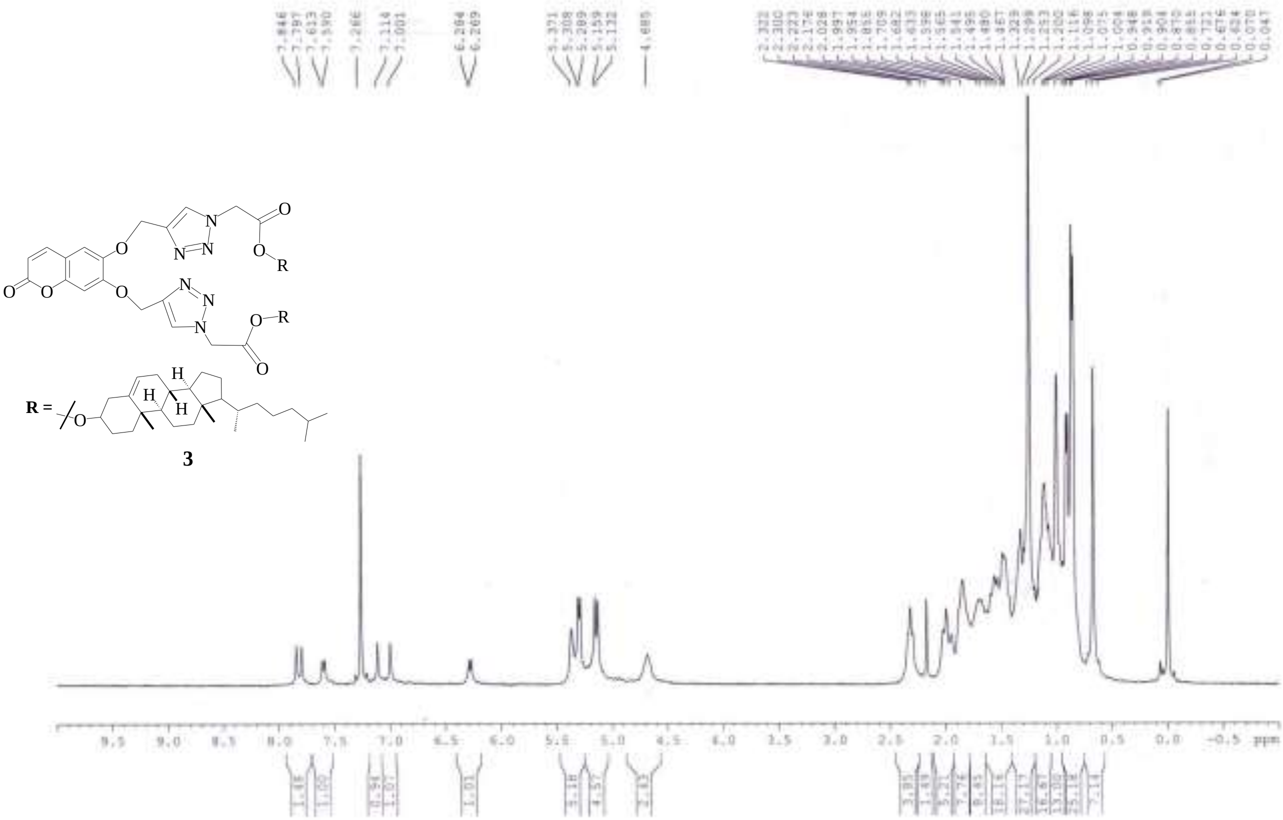

^{13}C NMR ($CDCl_3$, 100 MHz)

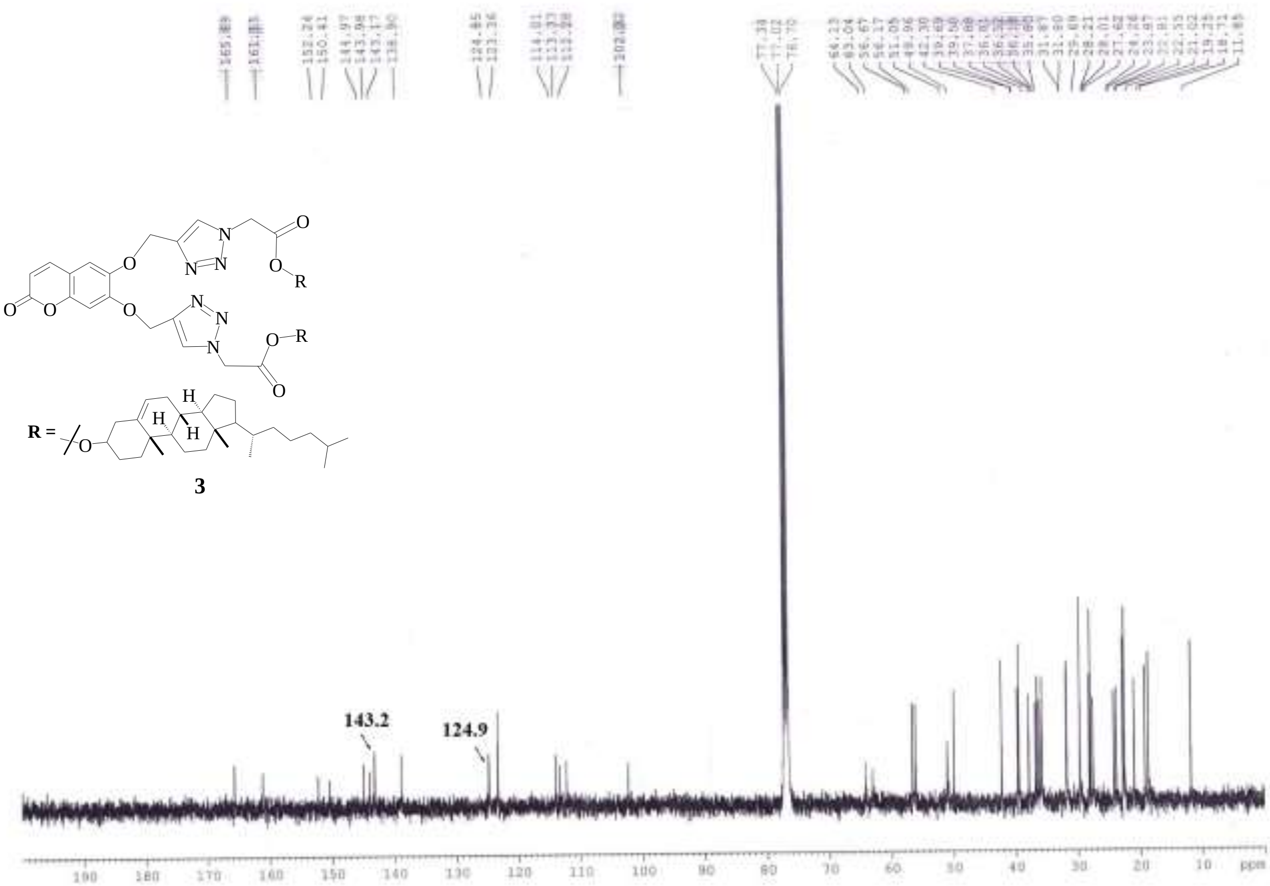

Mass spectrum of 3.